Synthesis of carbon nanotube/Ni nanocomposite film by electrophoresis and electroless deposition without Pd pretreatment

Masataka Hakamada *, Akitoshi Moriguchi, Satoshi Matsumura, Mamoru Mabuchi

Department of Energy Science and Technology, Graduate School of Energy Science, Kyoto University, Yoshidahonmachi, Sakyo, Kyoto 606-8501, Japan

ARTICLE INFO

ABSTRACT

Here we report the fabrication of carbon nanotubes (CNTs)/Ni nanocomposite film by electrophoretic deposition (EPD) and subsequent electroless deposition. The present technique requires no pretreatment with expensive Pd species for activation of the surface of CNTs. The EPD bath was modified with $NiSO_4 \cdot 6H_2O$ to form Ni clusters on the surface of CNTs. As a result, a thin Ni layer (6 nm thickness) was fabricated on CNTs, forming a CNT/Ni nanocomposite film with a thickness of 5–10 μm. The fabricated CNT/Ni film had nanoporous structure and exhibited electric double layer capacity and catalytic activities for decoloration of methyl orange.

© 2013 Elsevier B.V. All rights reserved.

1. Introduction

After the first report by Iijima [1], carbon nanotubes (CNTs) have drawn much attention, and have been used as a thin film for application to capacitors, actuators, and displays, for example [2]. Electrophoretic deposition (EPD) can be used to fabricate CNT thin films [3,4] with micrometer-scale thickness.

On the other hand, CNT/metal nanocomposites are emerging functional materials that have attracted enormous interest in recent years [4–9]. CNT/Ni powder is one of the most promising CNTs/metal nanocomposites, and has potential applications in capacitors [4,5], hydrogen storage [7,9], and hydrogenation catalysis [6,8]. Pretreatments of CNTs, such as activation by $PdCl_2$ [5–9], are necessary for Ni electroless deposition using the mild reducing agent $(CH_3)_2NHBH_3$ (DMAB). However, the high cost of $PdCl_2$ activator prevents the efficient production of these CNT/Ni nanocomposites.

Here we present the fabrication of CNT/Ni nanocomposite film by combining EPD and electroless deposition using DMAB without Pd-species pretreatments, and its electrochemical capacitance and catalytic activity were investigated.

2. Experimental procedures

2.1. Synthesis

Commercially available multi-walled CNTs (FloTube 9000, prepared by a catalytic vapor deposition process) were purchased from CNano Technology Ltd. The CNTs had an average diameter of 13 ± 3.5 nm and average length of 10 μm. The raw CNTs were treated in a concentrated mixture of nitric acid and sulfuric acid solutions at 333 K for 8 h. The treated CNTs were then washed several times to neutrality by ultrasonication (190 W, 90 min) in distilled water.

EPD was carried out to fabricate the CNT film [10] with modification of the bath by Ni addition. The negative and positive electrodes were Pt foils ($15 \times 25 \times 0.02$ mm^3). The distance between the electrodes was 20 mm. The EPD bath was composed of distilled water, the suspended acid-treated CNTs (200 mg/L) and $NiSO_4 \cdot 6H_2O$ (60 mg/L). A voltage of 30 V was applied between the electrodes at room temperature for 30 min. During the EPD, small amount of bubbles by water electrolysis was observed on both electrodes; a few macroscopic traces of bubbles were observed in the resulting CNT film. After EPD, the deposited CNT film (with 5–10 μm thickness) was washed with distilled water and dried in air. For comparison, EPD of CNT film without $NiSO_4 \cdot 6H_2O$ was also carried out.

After the EPD (with and without $NiSO_4 \cdot 6H_2O$), electroless deposition of Ni was carried out on the CNT film at 303 K. The electroless deposition bath was composed of $NiSO_4 \cdot 6H_2O$ (26.3 g/L), $Na_3C_6H_5O_7$ (29.4 g/L) and DMAB (3.0 g/L). pH of the bath solution was kept to 9 by using NaOH solution. The CNT film was immersed in the bath for

---

* Corresponding author. Tel.: +81 75 753 5427; fax: +81 75 753 5428.
E-mail address: hakamada.masataka.3x@kyoto-u.ac.jp (M. Hakamada).

40 min and stirred at 100 rpm. After the electroless deposition, the sample film was washed by distilled water and dried in air.

The samples were observed by a scanning electron microscope (SEM, SU6600 by Hitachi High-Technology Corp., operated at an accelerating voltage of 20 kV) equipped with an energy-dispersive X-ray (EDX) spectrometer (by Bruker) with a collecting angle of 35° and standard analysis period (<60 s), and analyzed by X-ray diffraction (XRD, X'Pert Pro by PANalytical, operated under a standard focusing beam configuration with Cu radiation).

2.2. Cyclic voltammetry

Cyclic voltammetry (CV) was conducted using a potentiostat and a typical three-electrode electrochemical cell with a Pt plate as a counter electrode, a saturated calomel electrode (SCE) as a reference electrode, and the sample as a working electrode in 6 mol/L KOH aqueous solution. CV was conducted at 30 mV s^{-1} in a potential range of −0.2 to −1.2 V vs. SCE. Samples analyzed were the CNTs/Ni nanocomposite film fabricated as explained above and CNT film (processed by EPD with NiSO$_4$·6H$_2$O and not followed by Ni electroless deposition). Both CNT/Ni and CNT films were used with Pt foil substrate as working electrodes. Potentials are shown based on SCE potential unless otherwise stated.

2.3. Decoloration of methyl orange solution

Methyl orange (MO), a typical azo dye used in the textile industry, is very stable. Different samples (CNT/Ni nanocomposite film, CNT film processed by EPD (without Ni electroless deposition) and Ni electroless deposition film) with nominal exposed areas of 7.5 cm^2 were immersed into 5 mL of MO solution (5 mg/L) at room temperature. The samples were immersed together with the Pt foil substrate. The experiments were conducted under dark conditions to distinguish the MO decrease from photocatalysis. The masses of CNTs used (1.2 mg) were the same for the CNT/Ni nanocomposite and the CNT film. The color of the solution was checked after 1 week from the immersion of the sample in MO solution.

3. Results and discussion

3.1. Characterization

The CNT film processed by EPD with NiSO$_4$·6H$_2$O exhibited a rough surface (Fig. 1b), compared to acid-treated CNTs not deposited by EPD (Fig. 1a). EDX analyses detected a trace amount (up to 3 at.%) of Ni in the CNT film processed by EPD with NiSO$_4$·6H$_2$O, as shown in Fig. 1b. These results suggest that small clusters of Ni species adhered to the surface of the CNTs during EPD. It is surmised that acid-treated

CNTs efficiently adsorbed Ni^{2+} and that the CNTs, positively charged by the Ni^{2+}, were then transported toward the negative electrode [4].

SEM observations exemplified in Fig. 1c demonstrated that the overall CNT network in the films was coated by a thin Ni layer by the electroless deposition carried out on the sample shown in Fig. 1b. The average diameter of the ligaments after Ni electroless deposition was 25 ± 9.6 nm, indicating that the electroless deposition increased the ligament diameters by a 6 nm layer. EDX also detected approximately 10 at.% of Ni, as shown in Fig. 1c. XRD analyses of the CNT/Ni nanocomposite film (Fig. 2) showed a broad 111 peak of metallic Ni at 44.5°. This suggests that the 6-nm-thick layer deposited on the surface of CNTs by the electroless deposition was metallic Ni.

On the other hand, the CNT film fabricated by EPD without NiSO$_4$·6H$_2$O addition was not accompanied by Ni clusters (Fig. 3a). In this case, without Ni clusters, Ni electroless deposition on the CNT film was unsuccessful even after 90-min immersion in the electroless deposition bath (Fig. 3b). Thus, NiSO$_4$·6H$_2$O in the EPD bath was crucial for subsequent Ni electroless deposition on CNTs.

In most cases when Ni is deposited on CNTs by electroless deposition, pretreatment with Pd species is required for surface activation [5,6]. However, in the present study, a Ni thin layer was deposited on the CNTs using the Ni clusters (Fig. 1c) instead of Pd pretreatment. That is, the clusters of Ni species (Fig. 1b) served as catalytically active points for subsequent Ni electroless deposition by DMAB. The Ni clusters were easily formed on the CNTs by simple addition of NiSO$_4$·6H$_2$O to the EPD bath solution. Hence, this EPD bath with NiSO$_4$·6H$_2$O will reduce the production costs of CNT/Ni nanocomposite films owing to the nonuse of Pd catalysts.

3.2. Properties

The microstructure of the CNT/Ni nanocomposite film was similar to that of nanoporous Ni [11] fabricated by dealloying. Hence, the surface effect on the properties of CNT/Ni was expected to be quite large because of its fine nanoporous structure [12–14]. Furthermore, the misfit straining due to lattice mismatch between CNTs and Ni may differentiate the properties of the deposited Ni in the CNT/Ni nanocomposite film from those of nanoporous Ni.

CV was conducted under the control of a potentiostat and a typical three-electrode electrochemical cell. As shown in Fig. 4, the shapes of the CV curves of both samples were similarly rectangular in the range of −1.0 to −0.3 V, indicating the capacitive behaviors of both samples. Much higher current was detected in the CNT/Ni nanocomposite film than in the CNT film without Ni electroless deposition. The capacitances calculated from the current [4] in the range of −1.0 to −0.3 V were 90 F/g$_{CNT}$ for the CNT/Ni nanocomposite film and 30 F/g$_{CNT}$ for the CNTs without Ni electroless deposition. Thus, Ni electroless deposition increased the capacitance of CNT film by three times.
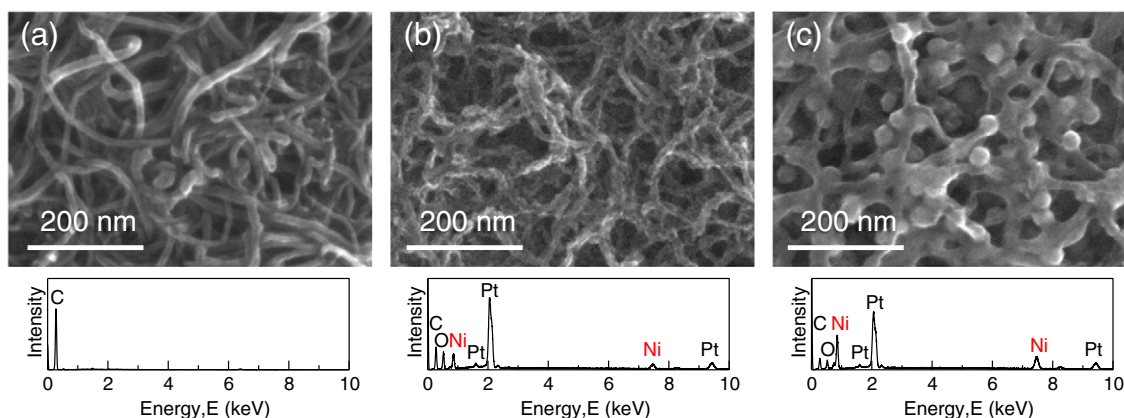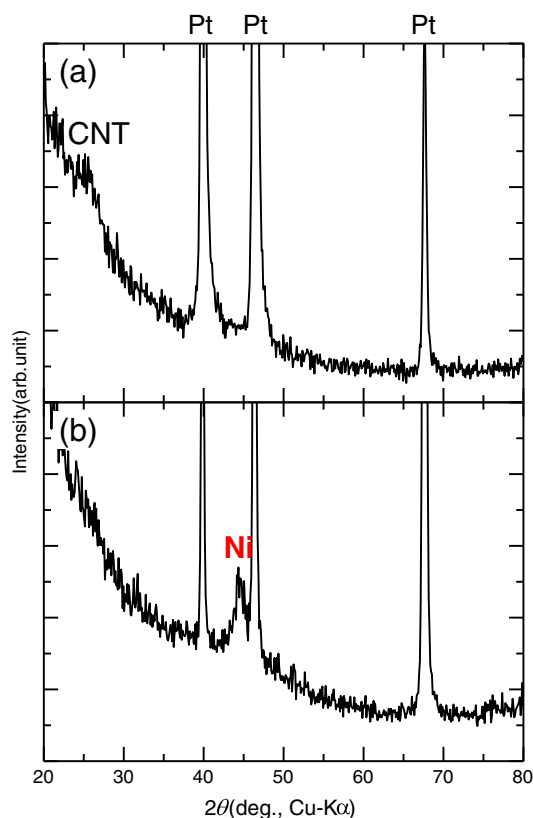

Fig. 1. SEM images and EDX results of (a) acid-treated CNTs (not deposited by EPD), (b) CNT film after EPD with NiSO$_4$·6H$_2$O and (c) CNT/Ni nanocomposite film.

Fig. 2. XRD patterns of (a) CNT film (without Ni electroless deposition) and (b) CNT/Ni nanocomposite film.

In general, the electric capacitance (C) depends on the permittivity (ε), thickness of the electric double layer (l), and electrode surface area (s) as follows.

$$C = \int \frac{\varepsilon}{4\pi l} ds. \tag{1}$$

The s of the CNT/Ni nanocomposite film was essentially quite similar to that of the CNT film without Ni electroless deposition, because the Ni electroless deposition homogeneously coated the surface of CNTs with a
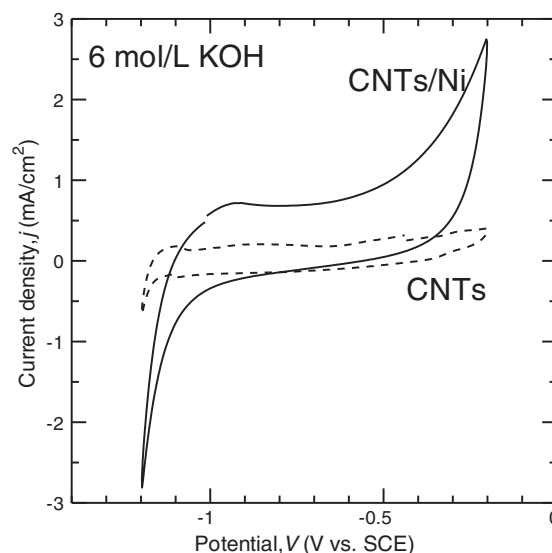

Fig. 4. CV curves of CNT film (without Ni electroless deposition) and CNT/Ni nanocomposite film in 6 mol/L KOH at a scan rate of 30 mV/s.

Ni thin layer (Fig. 1c). Thus, the ε and l were modified by the Ni electroless deposition, resulting in the observed improved electric capacitance. The strained lattice in the Ni nanoporous structure and its misfit with CNTs may have modified the electronic state of electrode surface (and subsequently ε and l).

On the other hand, Hsieh et al. reported that Ni clusters with 30–50 nm in diameter on CNT electrodes enhanced capacitance up to 240 F/g_{CNT} [15]. In their report, the improved capacitance was attributed to pseudocapacitive behavior in Ni; in the present study, however, the redox peak pair was not observed (Fig. 4) and the capacitance was not as good as has been reported in the literature [15]. The size, density, and amount of Ni clusters are likely to crucially affect the capacitance.

Finally, the catalytic activities of the CNT/Ni nanocomposite for decoloration of MO solution were assessed. After the 1-week immersion of the CNTs/Ni nanocomposite film, the MO solution was perfectly decolored (Fig. 5a), while the solution was confirmed to still have color after 1-week immersion of CNTs and Ni electroless deposition film (Fig. 5b and c). These results suggest that the CNTs/Ni nanocomposite film possesses a high catalytic decoloration capacity for azo dye solution.
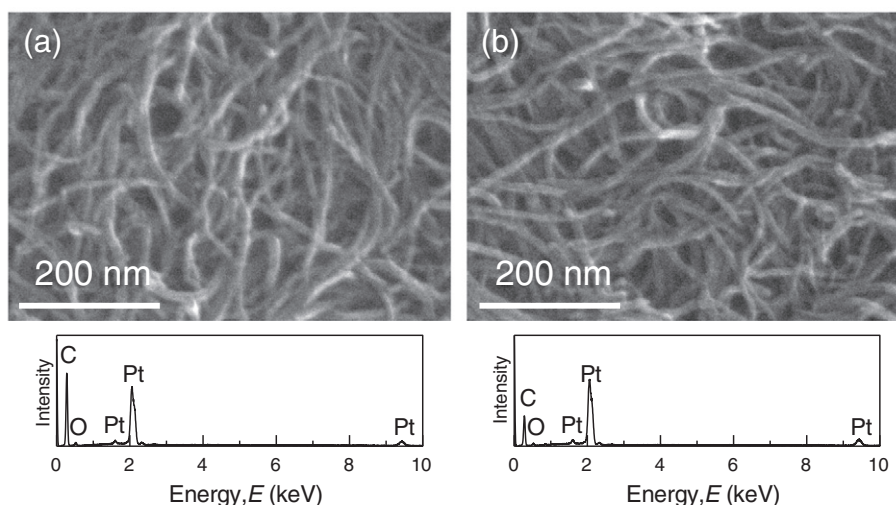
Fig. 3. SEM images and EDX results of (a) CNT film by electrophoretic deposition (EPD) without NiSO$_4$·6H$_2$O and (b) CNT film after unsuccessful Ni electroless deposition because of the absence of NiSO$_4$·6H$_2$O during the EPD.
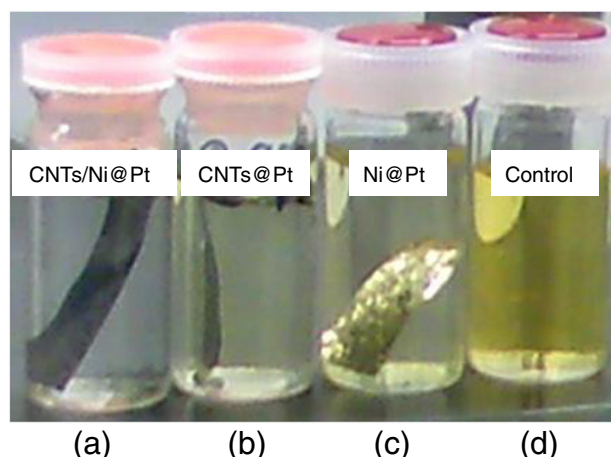
Fig. 5. Appearance of MO solution after 1-week immersion of (a) CNT/Ni nanocomposite film, (b) CNT film without Ni electroless deposition and (c) Ni electroless deposited film. All samples were deposited on Pt substrate foil. (d) Control MO solution with no sample.

To date, many studies have addressed the decoloration of MO for environmental issue solutions [16–20]. Typical photocatalysts such as TiO$_2$ can decompose MO under light irradiation [17]. However, the mechanism that governs the decoloration of MO solution by CNT/Ni nanocomposite film is different from photocatalysis because the experiments were conducted under dark conditions. The strained lattice of deposited Ni, which is caused by its nanoporous structure and misfit with CNTs, may be responsible for the observed MO decomposition [20].

4. Conclusions

In this study, we fabricated the nanoporous CNT/Ni nanocomposite film by the Ni-modified EPD and subsequent electroless deposition of Ni layer. During the EPD, small Ni clusters attached to the surface of CNTs, which promoted subsequent deposition of Ni layer on the CNTs during Ni electroless deposition. The present procedure for CNT/Ni nanocomposite films does not include costly Pd pretreatment for Ni electroless deposition; thus production costs will be greatly reduced.

The CNT/Ni nanocomposite film had nanoporous structure with three-dimensional Ni-coated CNTs network and exhibited electric double layer capacitance and catalytic decomposition of azo dyes (MO). The lattice strain in Ni induced by the nanoporous structure and misfit with substrate CNTs may cause these properties.

References

[1] S. Iijima, Nature 354 (1991) 56.
[2] L. Hu, D.S. Hecht, G. Gruner, Chem. Rev. 110 (2010) 5790.
[3] A.R. Boccaccini, J. Cho, J.A. Roether, B.J.C. Thomas, E.J. Minay, M.S.P. Shaffer, Carbon 44 (2006) 3149.
[4] M.-S. Wu, C.-Y. Huang, K.-H. Lin, Electrochem. Solid-State Lett. 12 (2009) A129.
[5] S.M. Bak, K.H. Kim, C.W. Lee, K.B. Kim, J. Mater. Chem. 21 (2011) 1984.
[6] S. Arai, Y. Imoto, Y. Suzuki, M. Endo, Carbon 49 (2011) 1484.
[7] K.-Y. Lin, W.T. Tsai, J.-K. Chang, Int. J. Hydrogen Energy 35 (2010) 7555.
[8] Z. Liu, Z. Li, F. Wang, J. Liu, J. Ji, K.C. Park, M. Endo, Mater. Res. Bull. 47 (2012) 338.
[9] C.-Y. Chen, K.-Y. Lin, W.-T. Tsai, J.-K. Chang, C.-M. Tseng, Int. J. Hydrogen Energy 35 (2010) 5490.
[10] B.J.C. Thomas, A.R. Boccaccini, M.S.P. Shaffer, J. Am. Ceram. Soc. 88 (2005) 980.
[11] M. Hakamada, M. Mabuchi, J. Alloy. Compd. 485 (2009) 583.
[12] M. Hakamada, M. Takahashi, T. Furukawa, M. Mabuchi, Appl. Phys. Lett. 94 (2009) 153105.
[13] M. Hakamada, M. Takahashi, T. Furukawa, M. Mabuchi, Philos. Mag. 90 (2010) 1915.
[14] M. Hakamada, S. Matsumura, M. Mabuchi, Mater. Lett. 70 (2012) 132.
[15] C.-T. Hsieh, Y.-W. Chou, W.-Y. Chen, J. Solid State Electrochem. 12 (2008) 663.
[16] R. Patel, S. Suresh, J. Hazard. Mater. B137 (2006) 1729.
[17] L. Sun, C. Tian, L. Wang, J. Zou, G. Mu, H. Fu, J. Mater. Chem. 21 (2011) 7232.
[18] A.D. Bokare, R.C. Chikate, C.V. Rode, K.M. Paknikar, Appl. Catal. B 79 (2008) 270.
[19] Y.-J. Xu, Y. Zhuang, X. Fu, J. Phys. Chem. C 114 (2010) 2669.
[20] J.-Q. Wang, Y.-H. Liu, M.-W. Chen, G.-Q. Xie, D.V. Louzguine-Luzgin, A. Inoue, J.H. Perepezko, Adv. Funct. Mater. 22 (2012) 2567.